**Supporting Information**

# Micromotor-based On-Off Fluorescence Detection of Sarin and Soman

Virendra V. Singh, Kevin Kaufmann, Jahir Orozco, Jinxing Li, Michael Galarnyk, Gaurav Arya, Joseph Wang*

## Experimental:

### 1.1 Synthesis of FLA/Si-$NH_2$/Pt micromotors

The FLA coated Janus micro motors were prepared using Supel™ Sphere silica-$NH_2$ particles (45 μm, Sigma-Aldrich, USA). In order to prepare FLA coated silica Janus micromotors, first the Fluoresceinamine (0.5mM) was dissolved in distilled water. Thereafter, silica particle was impregnated with FLA solution using the incipient wetness technique. This technique allows the FLA solution to just wet the adsorbent and be completely adsorbed on solid adsorbent. Thus prepared material was dried at 70°C for 1 h, and then washed with distilled water several times in order to remove any unbound FLA. After washing, the material was again dried at 70°C for 1 h and then used for the fabrication of micromotors. 0.005 g of the FLA coated silica particles were dispersed in 100 μL isopropanol, which was then pipetted onto glass slides and dried under room temperature. The FLA coated silica particles were coated with a Pt layer using a Denton Discovery 18 sputter system. The deposition was performed at room temperature with a DC power of 200 W and an Ar pressure of 2.5 mT for 30 s. In order to obtain a uniform Janus half-shell coating, rotation was turned off and the sample slides were set up at an angle to be parallel to the Pt target.

### 1.2 Propulsion of Janus motor

The propulsion of FLA coated silica micromotors in aqueous solution was performed in different SDS and hydrogen peroxide solutions until a final concentration of 1% SDS (Sigma-Aldrich, USA) and 2% hydrogen peroxide (Sigma-Aldrich USA) was determined to be optimal. Videos were captured by an inverted optical microscope (Nikon Eclipse Instrument Inc. Ti-S/L100), coupled with 20 X and 10 X objectives, a Hamamatsu digital camera C11440, and NIS Elements AR 3.2 software. The speed of the micromotors was tracked using an NIS Elements tracking module.

### 1.3 Fluorescent measurement of chemical warfare agent simulant DCP

For micromotor based detection experiments, DCP was added into 600 μl aqueous solution containing different numbers of FLA/Silica-$NH_2$/Pt micromotor ($0.5\times10^4$ to $2\times10^4$ motors/ml) with 1% SDS and 2% hydrogen peroxide as propulsion medium. Fluorescence measurements of the micromotors were acquired with a fluorescence imaging system. Stock solutions ($1\times10^{-1}$M to $1\times10^{-6}$M for DCP and 0.5mM for Fluoresceinamine) were prepared daily in double distilled water and subsequently diluted to the required concentration. Fluorescence emission spectra were acquired with a spectro-fluorometer at 490-nm excitation and emission between 510 and 610 nm using a green filter.

### 1.4 Fluorescence Microscopy.

Images and videos were captured using a CoolSNAP HQ2 camera, 20X objective (unless mentioned otherwise) and acquired at a frame rate of 10 frames/s using the Metamorph 7.1 software (Molecular Devices, Sunnyvale, CA). A Nikon Eclipse 80i upright microscope with B2-A FLA filter was used to capture fluorescence images and videos. The obtained mean fluorescence-intensity values (n=3) were corrected with the cameras' gain control and plotted as arbitrary units in all graphs depicting fluorescence.

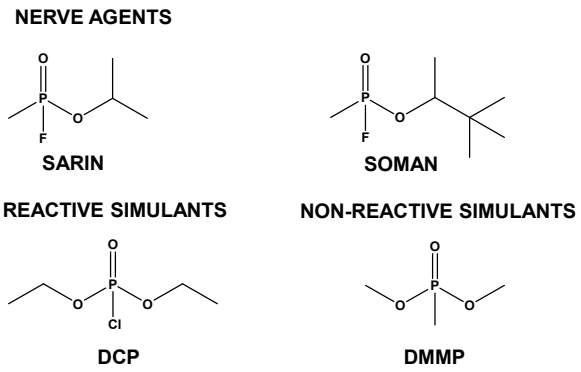


**Figure S1.** Structures of nerve agents and the simulant compounds utilized in this study.

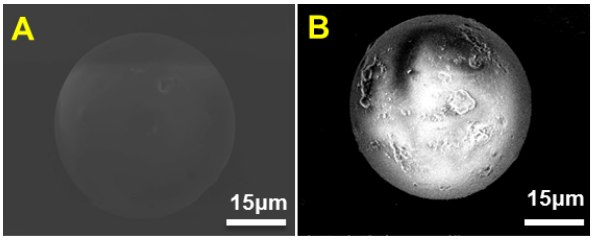


**Figure S2.** Scanning electron microscopy (SEM) image of silica before (A); and after loading of FLA (B).

| | **Atomic (%)** | |
|---|---|---|
| **Element** | **Before the coating** | **After the coating** |
| O | 45.54 | 36.56 |
| Si | 30.42 | 30.53 |
| N | 8.19 | 7.13 |
| C | 15.85 | 25.78 |
| **Total** | **100** | **100** |

**Figure S3.** Semi qualitative EDX analysis before and after FLA coating of silica-$NH_2$ particle.

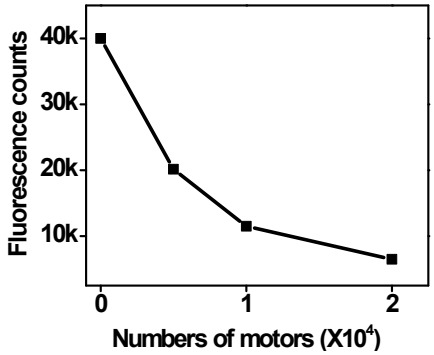


**Figure S4.** Effect of the number of micromotors on the efficient quenching of micromotors with DCP. Reaction Conditions: 600µL solution containing 1% SDS, 2% $H_2O_2$, and $10^{-3}$M DCP.

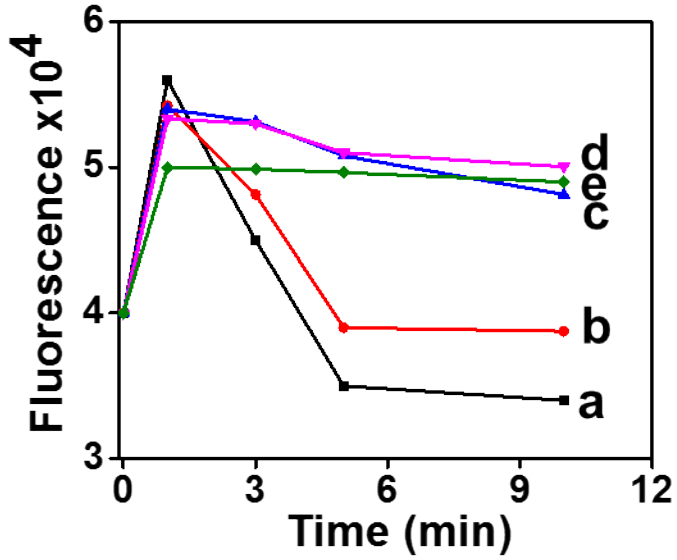


**Figure S5.** Time dependent fluorescent enhancement of micromotors in phosphate buffer pH 7.2 with different concentrations of DCP (a) $10^{-1}$ M (b) $10^{-2}$ M (c) $10^{-3}$ M (d) $10^{-4}$ M and (e) $10^{-5}$ M DCP Reaction conditions: $H_2O_2$ (2%), SDS (1%), $\lambda_{ex}$, 490 nm; $\lambda_{em}$ , 510 nm.

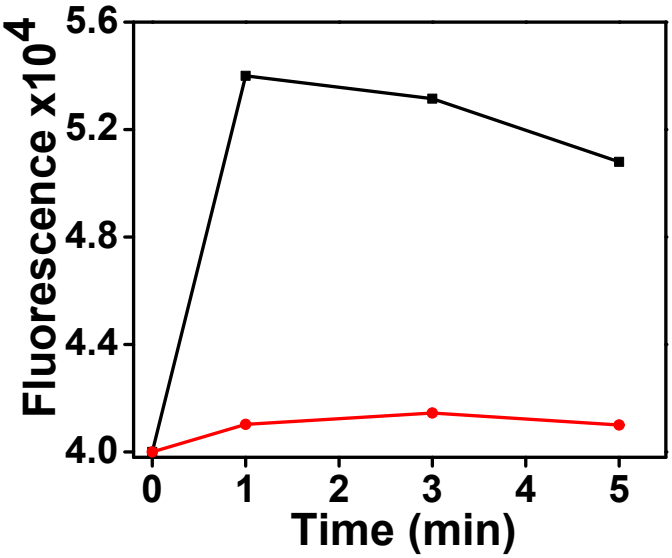


Figure S6. Micromotrs based detection of DCP in phospahte buffer pH 7.2: graph showing the movement of micromotors leading to rapid enhancement of fluorescence compared to static. Reaction conditions: conc. of DCP = $10^{-3}$M, $H_2O_2$ (2%), SDS (1%), and $2\times10^4$micromotors; $\lambda_{ex}$, 490 nm; $\lambda_{em}$, 510 nm.

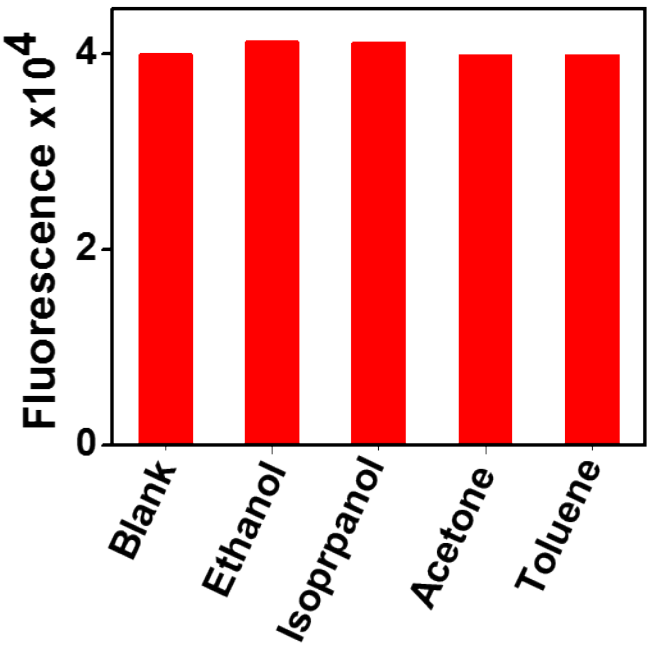


**Figure S7.** Interference study: Effect of common volatile organic compound on micromotor based fluorescent on/off or off/on Reaction conditions: Conc. of VOC $10^{-1}$ M, $H_2O_2$ (2%), SDS (1%), $\lambda_{ex}$, 490 nm; $\lambda_{em}$ , 510 nm.

## Simulation studies

It is observed that the mobile micromotors remain dispersed within the bulk solution while the static motors tend to sediment and form a densely packed layer at the bottom of the container. In such a scenario, each mobile motor can be modeled as a sphere of radius $R$ suspended within an infinite solution containing the analyte (species A) at a concentration $c_{A0}$ in the bulk (Fig. S1a). The analyte A reacts at the surface of the motor with the fluorophores (species F) with a surface rate $R_A$ (mol/cm$^2$/s) given by $R_A = -k_s c_A c_F$, where $k_s$ is a second-order reaction rate constant and $c_A$ and $c_F$ are the surface concentrations of species A and F at the motor surface, respectively. On the other hand, the sedimented layer of motors can be modeled as a planar sheet, also suspended in a solution of analyte A at bulk concentration $c_{A0}$ and reacting with the surface fluorophores with the abovementioned reaction rate (Fig. S1b). The reaction between DCP and fluorophores typically occurs rapidly[1], i.e., $k_s$ is very large, such that the concentration of the analyte A can be effectively assumed to be zero at the motor surface.

One can write down the governing mass-transfer equation (in spherical coordinates) for the concentration $c_A(r, t)$ of species A at radial distance $r$ from the center of the *suspended* micromotor and time $t$ [1]:

$$\frac{\partial c_A}{\partial t} = D_{AB} \frac{1}{r^2} \frac{\partial}{\partial r}\left( r^2 \frac{\partial c_A}{\partial r} \right), \qquad \ldots(1)$$

where $D_{AB}$ is the diffusivity of the analyte within the solution (species B). The two relevant boundary conditions and the initial condition are given by:

$$\begin{aligned} c_A &= 0 \quad @r = R \\ c_A &= c_{A0} @r \to \infty, \\ c_A &= c_{A0} @t = 0 \end{aligned} \qquad \ldots(2)$$

where $t = 0$ represents the time point when the motors are introduced into the solution. Note that we have ignored the convective term in the above model; we show later that the convective contribution arising from motor motion is much smaller than that due to diffusion and it can be estimated from mass-transport rates from diffusive alone. It should be noted that the *sedimented* layer of motors can be treated similarly by invoking the limit $R \to \infty$ in the final closed-form solution of above equation so as to model a planar reacting surface.

By implementing the following variable changes[2], $u = (c_{A0} - c_A)/r$ and $\eta = (r - R)/(4D_{AB}t)^{1/2}$, it is possible to convert the above governing equation, a partial differential equation (PDE) in two variables, into a PDE in one variable

$$\frac{\partial^2 u}{\partial \eta^2} + 2\eta \frac{\partial u}{\partial \eta} = 0, \qquad \ldots(3)$$

with the following two boundary conditions:

$$\begin{aligned} u &= c_{A0} R \quad @\eta = 0 \\ u &= 0 \qquad @\eta \to \infty \end{aligned}. \qquad \ldots(4)$$

The above PDE can be solved to yield the following solution for the concentration profile:

$$c_A = c_{A0} - c_{A0} \frac{R}{r}\left(1 - \mathrm{erf}\left(\frac{r - R}{2\sqrt{D_{AB} t}}\right)\right), \qquad \ldots(5)$$

The concentration profile can be used to obtain the molar flux $N_{AR}$ of analyte reacting at the motor surface by evaluating $N_{AR} \equiv -D_{AB}\, dc_A/dr$ at the surface $r = R$:

$$N_{AR} = D_{AB} c_{A0}\left[\frac{1}{R} + \frac{1}{\sqrt{\pi D_{AB} t}}\right] \qquad \ldots(6)$$

The above expression demonstrates how the surface reaction rate $N_{AR}$ (per unit area) increases as the size of the particles $R$ becomes smaller and how this reaction rate also decreases with time due to the flattening of the concentration profile with time.

Equation (6) can be used to determine the relative enhancement $E_{rate}$ in the reaction rate of the suspended mobile motors (of radius $R$) as compared to the sedimented static motors (of infinite radius $R \to \infty$):

$$E_{\text{rate}} \equiv \frac{N_{AR}(R)}{N_{AR}(R \to \infty)} = 1 + \sqrt{\frac{\pi D_{AB} t}{R^2}}. \qquad \ldots(7)$$

The diffusivity of the analyte (DCP in our case) may be estimated from the Wilke-Change correlation[3]:

$$D_{AB} = \frac{7.4 \times 10^{-8} (\Phi_B M_B)^{0.5} T}{\mu_B V_A^{0.6}} \qquad \ldots(8)$$

where $T$ is the absolute temperature (in Kelvin), $V_A$ is the molal volume (in $cm^3$/mol) of the solute (DCP) at normal boiling point,

and $M_B$, $\mu_B$, and $\Phi_B$ are the molecular weight (in g/mol), shear viscosity (in centipoise), and "association" factor of the solvent (water). Using the following parameter values: $T$ = 293 K, $M_B$ = 18 g/mol, $\mu_B$ = 1.0 cP, $\Phi_B$ = 2.26, and $V_A$ = 169.7 cm$^3$/mol (estimated from G. Le Bas' atomic volumes[4]), we obtain a diffusivity of $D_{AB} \approx 6.35 \times 10^{-6}$ cm$^2$/s. Using this diffusivity estimate along with $R \approx 22.5$ $\mu$m as the size of our Janus silica micromotors, we obtain a reaction rate enhancement of $E_{rate} = 1 + 1.99\sqrt{t}$, which increases from a factor of 1 to about 50 within the first 10 minutes of introducing the micromotors into the analyte solution.

Note that while the enhancement in *reaction rate* of mobile over static motors increases with time, the absolute reaction rate of mobile motors (and static ones) keeps decreasing with time following Eq. (6). The enhancement in the *overall* amount of analyte consumed by the motors is therefore actually smaller. The overall amount of analyte $W(t)$ consumed by the motors (per unit area) from time $t$ = 0 to $t$ is given by

$$W(t) = \int_0^t N_{AR}(t)dt = D_A c_{A0}\left[\frac{t}{R} + \sqrt{\frac{4t}{\pi D_{AB}}}\right]. \qquad \ldots(9)$$

The enhancement $E_{net}$ in the net amount of analyte consumed by mobile motors relative to static motors is then given by

$$E_{net} \equiv \frac{W(R)}{W(R \to \infty)} = 1 + \sqrt{\frac{\pi D_{AB} t}{4R^2}} \qquad \ldots(10)$$

By using the earlier estimates of the diffusivity and motor size, we obtain $E_{net} = 1 + \sqrt{t}$ as the enhancement in the net amount of analyte consumed, which increases from 1 to about 25 within the first 10 minutes of introducing the micromotors into the analyte solution.

We recall that the above enhancements were estimated based on mass-transfer equations neglecting convection. It is possible to estimate mass-transfer (reaction rate) arising from convection relative to that arising from diffusion by computing the dimensionless Sherwood number Sh, which represents the ratio of convective mass transfer to diffusive mass transfer. The Sherwood number itself is related to the Reynolds number Re and the Schmidt number Sc via the relationship[1]:

$$\mathrm{Sh} = 2 + 0.664\,\mathrm{Re}^{1/3}\,\mathrm{Sc}^{1/2}, \qquad \ldots(11)$$

where $\mathrm{Re} = \rho U d/\mu$ and $\mathrm{Sc} = \mu/\rho D$. In these equations, $\rho$ and $\mu$ denote the density and viscosity of the fluid, $D$ denotes the characteristic diffusivity of the diffusing species, and $U$ and $d$ denote the characteristic velocity and characteristic length scale of the flow. For our micromotor system, $\rho$ = 1 g/cm$^3$, $\mu$ = 1 cP, $D = 6.35 \times 10^{-6}$ cm$^2$/s (from earlier analysis), $U$ = 145 $\mu$m/s (mean velocity of motors), and $d$ = 50 $\mu$m (diameter of micromotors). Using these parameters, we obtain Re = 0.00653 and Sc = 1575, and therefore Sh = 2.56. For static motors, with $U$ = 0, Sh = 2. Thus, the fold-enhancement in mass-transfer arising from the motion of micromotors is 2.62/2 = 1.31, i.e., an additional enhancement of ~30% arising from purely convective effects. Thus, the thickness of the boundary layer at the surface of the motors due to solvent flow around the motors is compatible with the characteristic diffusion length (typically on the order of $R$ for spherical particles), leading to only moderate additional enhancement in mass-transfer from convection on top of the mass-transfer due to diffusion.

We expect that the bubbles emanating from one half of the motors further enhanced mass transfer through mixing. However, the relative magnitude of mass transfer arising from such mixing is difficult to predict due to a lack of good models and unknown parameters.

## References


[1] J. R. Welty, C. E. Wicks, G. Rorrer, R. E. Wilson, *Fundamentals of momentum, heat, and mass transfer*. New York: John Wiley & Sons; 2009.

[2] S. Middleman, *An Introduction to Mass and Heat Transfer: Principles of Analysis and Design.* New York: Wiley; 1998.

[3] C. R. Wilke, P. Chang, *AIChE Journal*, 1955, **1**, 264-270.

[4] G. Le Bas, *The Molecular Volumes of Liquid Chemical Compounds, from the Point of View of Kopp*. London: Longmans; 1915.